



Universiteit  
Leiden  
The Netherlands

## **mRNA and drug delivery with lipid-based nanoparticles**

Zeng, Y.

### **Citation**

Zeng, Y. (2022, December 6). *mRNA and drug delivery with lipid-based nanoparticles*. Retrieved from <https://hdl.handle.net/1887/3492640>

Version: Publisher's Version

License: [Licence agreement concerning inclusion of doctoral thesis in the Institutional Repository of the University of Leiden](#)

Downloaded from: <https://hdl.handle.net/1887/3492640>

**Note:** To cite this publication please use the final published version (if applicable).

## **Chapter 5**

### **Lipid nanoparticle-based mRNA candidates elicit potent T cell immune responses**

## Abstract

The induction of a potent T cell response is essential for successful tumor immunotherapy and protection against many infectious diseases. In the past few years, mRNA vaccines have emerged as potent immune activators and inducers of a robust T cell immune response. The recent approval of the Moderna and the Pfizer/BioNTech vaccines based on lipid nanoparticles (LNP) encapsulating antigen-encoding mRNA has revolutionized the field of vaccines. The advantages of LNPs are their ease of design and formulation resulting in potent, effective, and safe vaccines. However, there is still plenty of room for improvement with respect to LNP efficacy, for instance, by optimizing the lipid composition and tuning LNP for specific purposes. mRNA delivery is known to be strongly dependent on the lipid composition of LNPs and the efficiency is mainly determined by the ionizable lipids. Besides that, cholesterol and helper lipids also play important roles in mRNA transfection potency. Here, a panel of LNP formulations was studied by keeping the ionizable lipids constant, replacing cholesterol with  $\beta$ -sitosterol, and changing the fusogenic helper lipid DOPE content. We studied the ability of this LNP library to induce antigen presentation and T cell proliferation to identify superior LNP candidates eliciting potent T cell immune responses. We hypothesize that using  $\beta$ -sitosterol and increasing DOPE content would boost the mRNA transfection on immune cells and result in enhanced immune responses. Transfection of immortal immune cell lines and bone marrow dendritic cells (BMDCs) with LNPs was studied. Delivery of mRNA coding for the model antigen ovalbumin (OVA-mRNA) to BMDCs with a number of LNP formulations, resulted in a high level of activation, as evidenced by the upregulation of the co-stimulatory receptors (CD40 and CD86) and IL-12 in BMDCs. The enhancement of BMDC activation and T cell proliferation induced by the introduction of  $\beta$ -sitosterol and fusogenic DOPE lipids were cell dependent. Four LNP formulations (C12-200-cho-10%DOPE, C12-200-sito-10%DOPE, cKK-E12-cho-10%DOPE and cKK-E12-sito-30%DOPE) were identified that induced robust T cell proliferation and enhanced IFN- $\gamma$ , TNF- $\alpha$ , IL-2 expression. These results demonstrate that T cell proliferation is strongly dependent on LNP composition and promising LNP-mRNA vaccine formulations were identified.

## Introduction

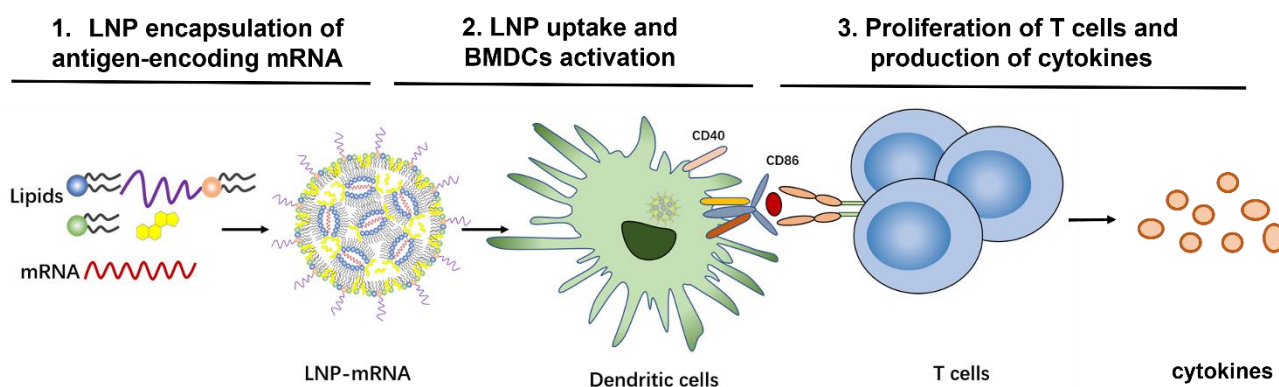
Messenger RNA (mRNA) is an intermediate genetic carrier that is used by organisms as a translational template; therefore, it can serve as a tool for protein expression by introducing exogenous mRNA into target cells.<sup>1</sup> The recent coronavirus pandemic dramatically accelerated the development of mRNA-based vaccines and also put a spotlight on other potential applications such as cancer immunotherapy, infectious disease vaccination, protein replacement, gene editing, and tissue engineering.<sup>2-5</sup> This surging interest and development of mRNA as a vaccine is driven by the following advantages: I) There is no potential infection or insertional mutagenesis risk as mRNA is a non-infectious, non-integrating genetic carrier;<sup>6</sup> II) mRNA is degraded by physiological metabolic pathways and the *in vivo* half-life can be tuned by the introduction of various chemical modifications and the delivery method;<sup>1, 7, 8</sup> III) *in vitro* transcription (IVT) enables rapid, inexpensive, and scalable industrial manufacturing of mRNA.<sup>2</sup> Combined these advantages contribute to the great promise of mRNA-based therapies for both infectious diseases and cancer.

Since mRNA is susceptible to degradation by nucleases *in vivo*, it needs to be protected from the environment upon administration. Furthermore, mRNA is unable to transfect cells and a drug delivery system is therefore required to overcome these problems. Thus, an ideal mRNA delivery system must protect against endonucleases, avoid rapid renal clearance, and promote cell entry of the tissue of interest.<sup>9, 10</sup> Lipid nanoparticles (LNPs) are the most advanced non-viral nucleic acid vector and the first RNA interference (RNAi) therapy, Onpattro, was approved in 2018 to treat hereditary amyloidogenic transthyretin amyloidosis (hATTRv).<sup>11</sup> LNPs are typically composed of 4 types of lipids: ionizable lipids, helper lipids, cholesterol, and PEGylated lipids. Each of these components is required to obtain stable LNPs with control over mRNA encapsulation efficiency, particle size, charge, and stability. Ionizable lipids are required to condense and protect the genetic cargo via electrostatic interactions and their chemical structure plays a crucial role in the resulting transfection efficiency. Helper lipids, cholesterol, and PEGylated lipids are required to control the LNP size as well as colloidal stability, and to minimize protein absorption.<sup>12, 13</sup> The two LNP-based vaccines against SARS-CoV-2 approved in 2020 are a milestone in mRNA-based therapeutics and accelerated the development of LNPs as a facile drug delivery tool for any nucleic acid-based therapy.<sup>14, 15</sup> LNPs have also been studied in cancer immunotherapy<sup>3, 16, 17</sup> and vaccination against infectious diseases, such as Zika virus,<sup>18, 19</sup> powassan virus,<sup>20</sup> HIV-1,<sup>21, 22</sup> and influenza virus.<sup>23-25</sup> In these studies, the immune response was interrogated mainly as a function of mRNA dose, but there is still room for improvement by optimizing the lipid composition of LNPs to achieve the desired cytotoxic T-cell production to mediate successful immunotherapy against many viral diseases and tumors.

For instance, replacing cholesterol with its analog  $\beta$ -sitosterol was reported to enhance the mRNA transfection efficiency.<sup>26</sup> Onpattro uses the lipid MC3 as the ionizable lipid, which was the first approved ionizable lipid for LNPs and showed effective gene silencing by delivering siRNA to hepatocytes.<sup>11, 27</sup> The two ionizable lipids, C12-200 and cKK-E12, were chosen for this study because they demonstrated to be more efficient in delivering siRNA as compared to MC3 and were also able to deliver mRNA, leading to potent immune responses in tumor immunotherapy.<sup>3, 28-30</sup> Helper lipids like 1,2-dioleoyl-*sn*-glycero-3-phosphoethanolamine (DOPE) can increase the fusogenicity of LNPs, aiding endosomal escape and cytosolic translation.<sup>31</sup> This is due to the fact that DOPE prefers to adopt an inverted hexagonal phase, which is assumed to be fusogenic, thereby promoting endosomal escape

resulting in enhanced transfection.<sup>32,33</sup>

To evaluate the effect of lipid composition on mRNA delivery, translation into proteins, antigen-presenting ability, and ultimately T-cell activation, we designed a library of LNPs by varying the lipid composition. In this study, the amount of the ionizable lipids (C12-200 and cKK-E12) and PEGylated lipid was kept constant, the replacement of cholesterol for  $\beta$ -sitosterol and different ratio of fusogenic lipid DOPE were studied to optimize the mRNA delivery efficiency. All studied LNPs induced in general high transfection of immortal cell lines regardless of the exact composition when encapsulating mRNA encoding a green fluorescent protein (EGFP-mRNA). Bone marrow dendritic cells (BMDCs) with a potent antigen-presenting capacity for stimulating naive, memory, and effector T cells were employed to evaluate the immune responses. In this study, mRNA which codes for the model immunology protein chicken ovalbumin (OVA-mRNA) was encapsulated in LNPs to activate BMDCs and stimulate T cell proliferation. BMDCs were highly activated and T cells were strongly proliferated after the internalization of OVA-mRNA-LNPs in a concentration-dependent manner (**Scheme 1**). Based on robust T cell proliferation and cytokine expression measurements, we obtained 4 efficient LNP candidates for future *in vivo* studies towards the development of superior LNP-mRNA formulation. This study provides evidence that the lipid composition optimization of LNPs is beneficial for maximizing T cell immune responses.



**Scheme 1.** Workflow to investigate the role of mRNA-LNP composition on T-cell activation and immune response.

## Results

### Design and characterization of LNPs

We previously showed that the silencing effect of siRNA using LNPs could be improved via tuning the internal LNP structure of the hydrophobic core from lamellar to inverse hexagonal by replacing DSPC with the fusogenic lipid DOPE in the LNP formulation, which is believed to be more fusogenic. In this study 1,2-dioleoyl-3-dimethylammonium-propane (DODAP) was used as the ionizable lipid. Inspired by this, we wondered whether mRNA transfection could also be enhanced by using other ionizable lipids. In the current study, two highly efficient ionizable lipids were used: C12-200 and cKK-E12. These ionizable lipids were efficient in siRNA delivery and the effective dose (ED<sub>50</sub>, C12-200~0.01 mg/kg, cKK-E12~0.002 mg/kg) was significantly lower than for MC3 (ED<sub>50</sub>~0.03 mg/kg). They also induced strong cytotoxic CD8<sup>+</sup> T cell responses against B16F10 melanoma tumors

after immunization with LNP containing OVA-mRNA, resulting in tumor shrinkage and extended overall survival of the treated mice.<sup>3, 28-30</sup> In a recent study, the cholesterol analog  $\beta$ -sitosterol was able to trigger enhanced mRNA transfection efficiency of LNPs in cancer cells compared to cholesterol due to the enhanced fragility, originating from an altered surface composition and shape,<sup>26</sup> and it was therefore included in our LNP library.

In this study, 10 LNP formulations were prepared, for which the ionizable lipids C12-200/cKK-E12 and the PEGylated lipid DMG-PEG2000 were kept constant at 50% and 1.5%, respectively. To study the effect of DOPE, its content varied from 10 to 49 mol% by replacing cholesterol (or its variant) (Fig. 1a-1b). All resulting LNPs had a comparable diameter ( $\sim 120$  nm) with a polydispersity index (PDI)  $< 0.20$  as determined by dynamic light scattering (DLS), as well as a near-neutral surface charge (Fig. 1c-1d). mRNA encapsulation efficiencies were also comparable for all LNPs and typically  $>80\%$  (Fig. 1e). Thus, replacing cholesterol with  $\beta$ -sitosterol or increasing DOPE did not change the physicochemical characteristics of the LNPs. The LNPs were stable for at least 1 month when stored at  $4^\circ\text{C}$  (SI Fig.1a-d).

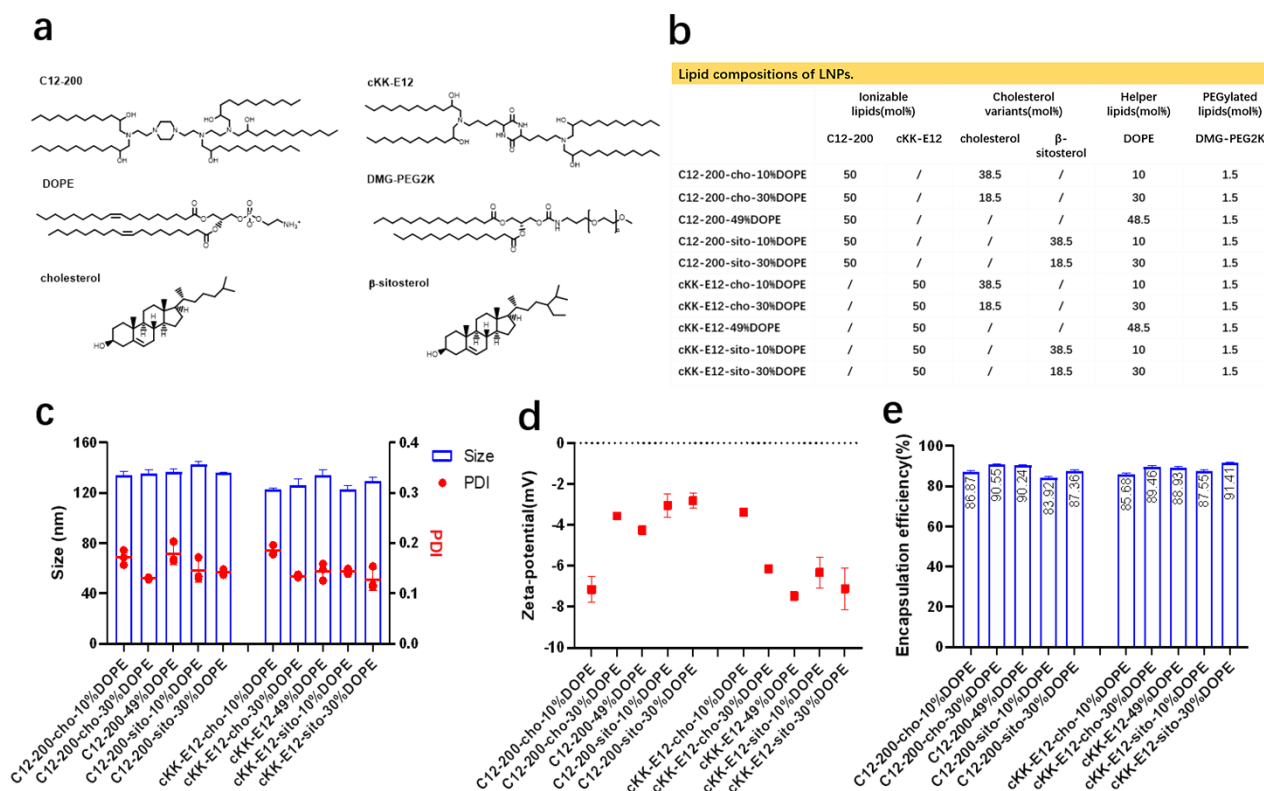


**Figure 1.** Design and characterization of different LNPs. (a) Lipids used in this study. (b) Lipid composition of LNPs. (c) Sizes and polydispersity index of LNPs as determined by DLS. (d) Zeta potential of LNPs determined by Laser Doppler Electrophoresis. (e) Encapsulation efficiency of OVA-mRNA in LNPs as determined by a Ribogreen RNA assay.

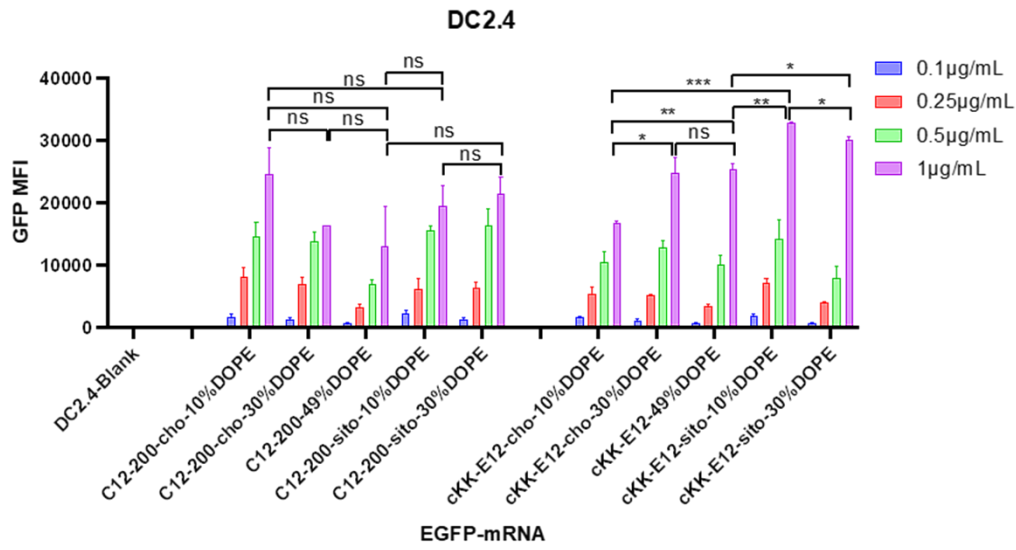
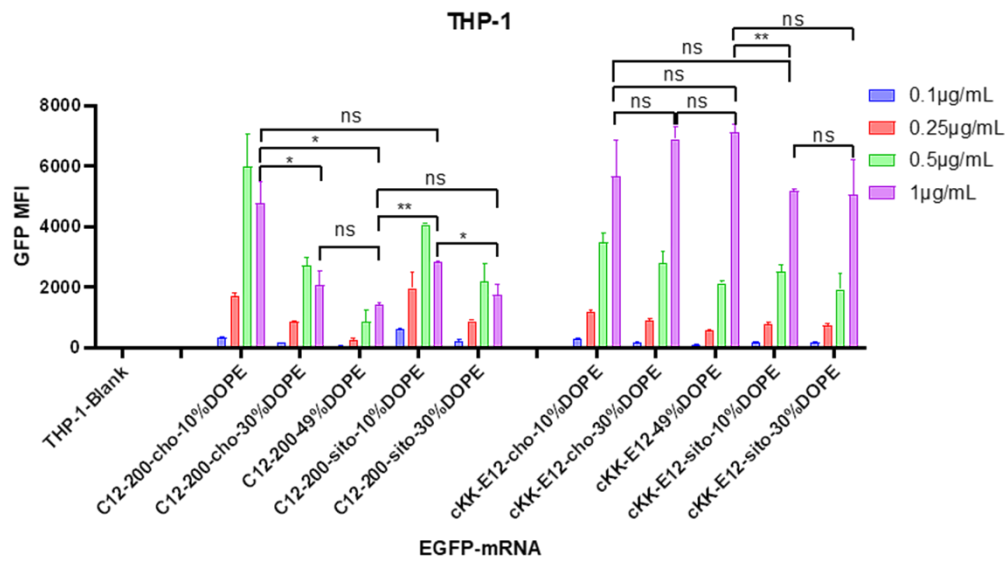
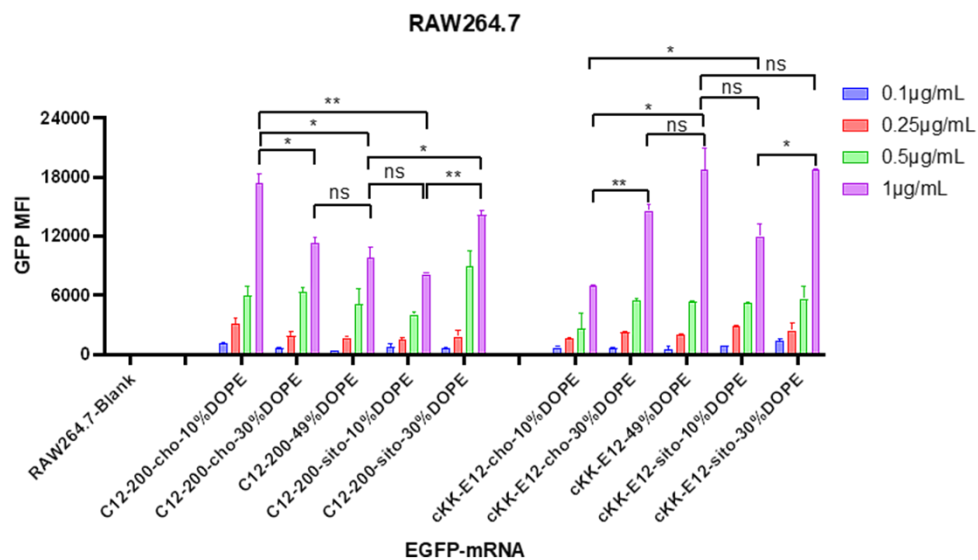
### Cell transfection efficiency

To study mRNA delivery and translation, EGFP-mRNA encoding for green fluorescent protein

(GFP) was encapsulated in the LNPs and the transfection efficiency was compared as a function of lipid composition in cervical carcinoma cells (HeLa) and Calu-3 cells.

Firstly, when comparing the transfection efficiency of different ionizable lipids, both C12-200 and cKK-E12 induced enhanced mRNA transfection efficiency on HeLa and Calu-3 as compared to MC3 (**SI Fig. 2a-b**). This is not unexpected as MC3 was designed for siRNA delivery while the mRNA delivery efficiency was less efficient.<sup>11, 27</sup> Maximum transfection of HeLa cells was obtained with an EGFP-mRNA concentration of 0.5  $\mu\text{g}/\text{mL}$  for all LNPs. In Calu-3 cells, the GFP expression of most LNPs increased with increasing EGFP-mRNA concentrations. Next, the effect of replacing cholesterol with  $\beta$ -sitosterol was studied. The introduction of the latter sterol significantly enhanced GFP expression for LNPs with MC3 as the ionizable lipid in both cell lines. When cKK-E12 was included in the LNPs, GFP expression was only enhanced in HeLa cells, while for C12-200-based LNP formulations no enhancement was observed at all. Finally, we studied whether increasing amounts of DOPE would enhance mRNA delivery and concomitant GFP expression. However, no general trend could be deduced from changing the DOPE ratio in LNP. Thus, we only observed a modest increase in transfection efficiency by replacing cholesterol with  $\beta$ -sitosterol.

Next, antigen-presenting cells (DC2.4) and macrophage cells (THP-1 and RAW264.7) were studied to evaluate the LNP-mRNA transfection performance on immortal cells mediating immune responses. Since LNPs with C12-200 and cKK-E12 as the ionizable lipids exhibited significantly higher transfection than MC3 containing LNPs, we continued this study with C12-200 and cKK-E12 only. In general, LNPs containing cKK-E12 induced a higher GFP expression than LNPs with C12-200 in three cell lines used (**Fig. 2a-2c**). On the other hand, introduction of  $\beta$ -sitosterol increased the transfection efficiency of the cKK-E12 LNPs in DC2.4 and RAW264.7, but not for C12-200 LNPs. When cholesterol was replaced by increasing amounts of DOPE, no transfection enhancement was observed for C12-200 LNPs. In contrast, enhanced transfection efficiency of cKK-E12 LNPs was observed in all tested cell lines. However, transfection enhancement was observed in DC2.4, and RAW264.7 cells when cKK-E12 LNPs contained  $\beta$ -sitosterol, but not in THP-1 cells (**Fig. 2a-2c**). Confocal microscopy imaging was used to visualize GFP expression and concomitant strong fluorescence intensity, and almost every cell produced strong and uniform GFP expression. In contrast, transfection with the commercial mRNA transfection reagent lipofectamine message MAX (lipofectamine) resulted in only a few fluorescent cells in the DC2.4 cell line (**Fig. S3**). In summary, all LNPs with either C12-200 or cKK-E12 as the ionizable lipid induced efficient transfection on immortal immune cell lines; however, the transfection efficiency enhancement by both the  $\beta$ -sitosterol replacement and the fusogenic helper lipid DOPE ratio increase was dependent on the cell line used.

**a****b****c**

**Figure 2.** Transfection efficiency of LNPs after encapsulating EGFP-mRNA on immortal immune cell lines. The GFP expression fluorescence intensity (GFP MFI) of LNPs within (a) DC2.4 cells, (b) THP-1 cells, and (c) RAW264.7. Data are presented as mean  $\pm$  sd. Statistical significance was calculated by unpaired student t-test on 1  $\mu$ g/mL. (\*\*\*\*,  $P < 0.0001$ , \*\*\*,  $P < 0.001$ , \*\*,  $P < 0.01$ , \*,  $P < 0.05$ , ns, no significant difference,  $n = 3$ )

### **BMDC transfection with EGFP-mRNA**

As APC cell lines provided mixed results, we next investigated primary APCs. As the next step towards both efficient intracellular antigen expression and subsequent immune cell activation to generate a robust immune response, the transfection efficiency of EGFP-mRNA loaded LNPs in BMDCs was investigated. Confocal microscopy imaging showed that all LNP formulations induced effective intracellular mRNA delivery to BMDCs, and performed better than the commercial transfection reagent Lipofectamine (**Fig. 3a**).  $\beta$ -Sitosterol boosted the transfection efficiency of the LNPs with cKK-E12 as the ionizable lipids but not for C12-200 (**Fig. 3b**). Finally, replacing cholesterol with DOPE did not enhance the GFP expression of either C12-200 and cKK-E12 LNPs (**Fig. 3b**).

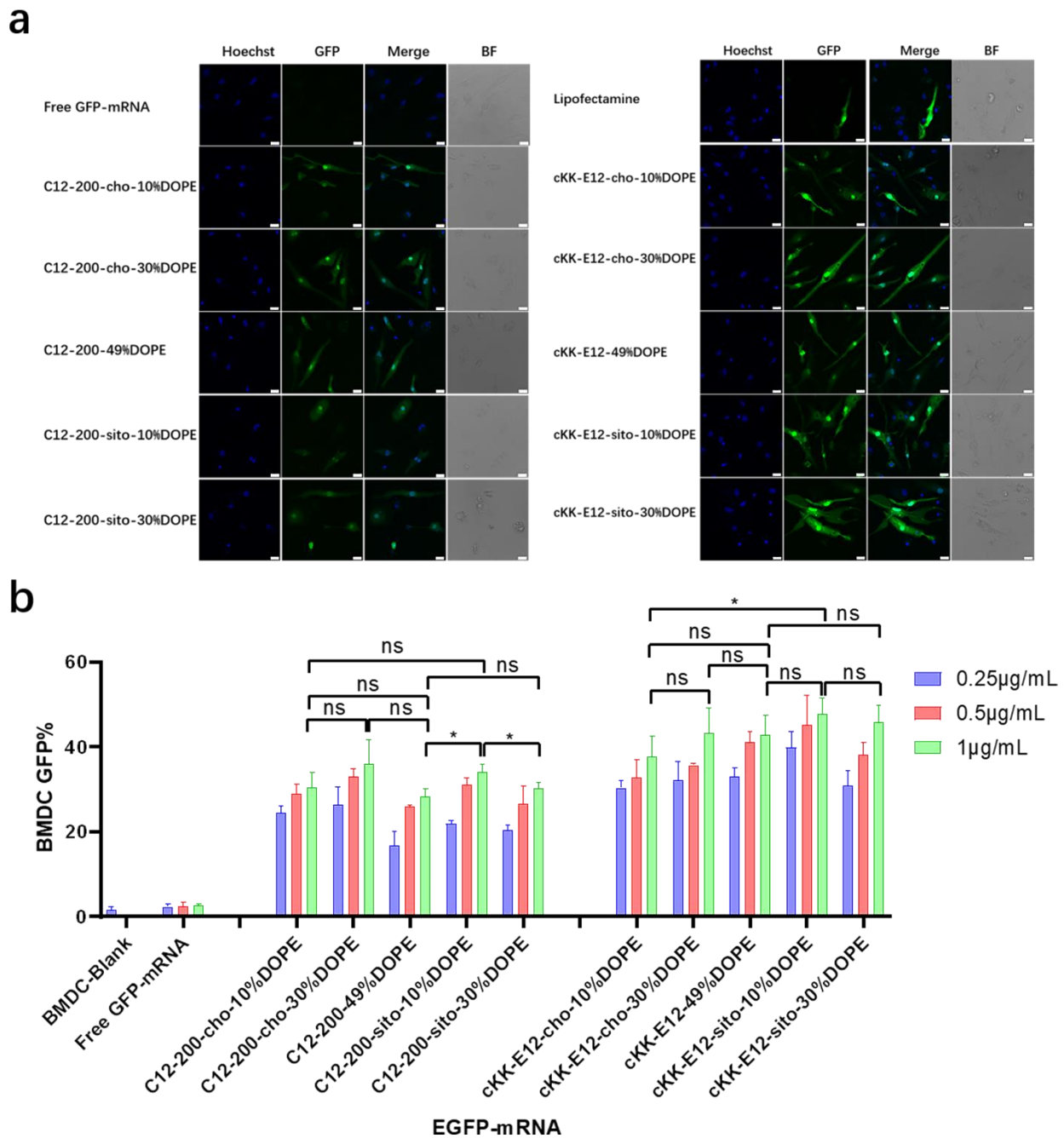


**Figure 3.** Transfection efficiency of LNPs after encapsulating EGFP-mRNA on BMDC cells. **(a)** Confocal images of the EGFP-mRNA transfection of LNPs on BMDC cells, EGFP-mRNA concentration was 0.5 µg/mL, incubated 24 h. Scale bar is 20 µm. **(b)** The GFP positive percentages of LNPs by flow cytometry analysis on BMDC cells of different EGFP-mRNA concentrations after 24 h incubation. Data are presented as mean ± sd. Statistical significance was calculated by unpaired student t-test on 1 µg/mL. (\*\*\*\*,  $P < 0.0001$ , \*\*\*,  $P < 0.001$ , \*\*,  $P < 0.01$ , \*,  $P < 0.05$ , ns, no significant difference,  $n = 3$ )

### Activation of BMDCs

Effective mRNA vaccination demands both efficient intracellular expression and subsequent APC activation to generate a robust immune response.<sup>16</sup> The model antigen chicken ovalbumin protein has been widely applied to evaluate the immune response, thus mRNA encoding ovalbumin (OVA-

mRNA) formulated in the LNPs was employed to activate BMDCs. The activation of BMDCs results in elevated expression of surface costimulatory molecules such as CD40, and CD86. To test APC activation induced by LNPs, we treated naïve BMDCs for 24 h with LNPs containing OVA-mRNA. All LNPs managed to produce increased expression of CD40 and CD86 compared to nontreated BMDCs or incubated with free OVA-mRNA, which indicates successful BMDC activation (**Fig. 4a-4b**). Both positive percentage and fluorescence intensity comparisons of CD40 and CD86 revealed no significant differences between C12-200 LNP formulations. Furthermore, neither the introduction of DOPE nor  $\beta$ -sitosterol at the expense of cholesterol boosted BMDC activation (**Fig. 4a-4b**, **SI Fig. 4a-4b**). For LNPs with cKK-E12, we observed that cKK-E12-cho-10%DOPE and cKK-E12-sito-30%DOPE induced a stronger upregulation of CD40 and CD86 expression (**SI Fig. 4a-4b**).

The activation of dendritic cells often promotes inflammatory cytokine gene expression. We, therefore, examined cytokine IL-12 (p70) expression in the supernatant of BMDCs. Interleukin-12 (IL-12) is a heterodimeric pro-inflammatory cytokine that regulates T helper 1 (Th1) and CD8<sup>+</sup> T-cell responses, and is mainly produced by dendritic cells and phagocytes in response to pathogens during infection.<sup>34</sup> Compared to blank BMDCs and free OVA-mRNA, all LNPs mediated superior IL-12 (p70) production (**Fig. 4c**); however, no significant differences among the tested LNPs were observed. The cell viability of BMDCs was determined to ensure that the LNPs were non-toxic at the concentrations used. All LNP formulations showed no detectable cytotoxicity (cell viability > 60%), even at a high concentration (1  $\mu$ g/mL), revealing that these LNPs are indeed non-toxic (**Fig. 4d**).

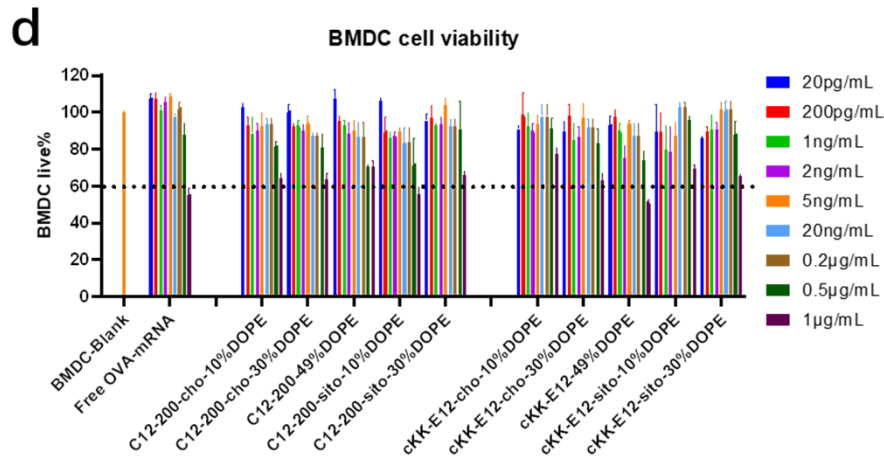
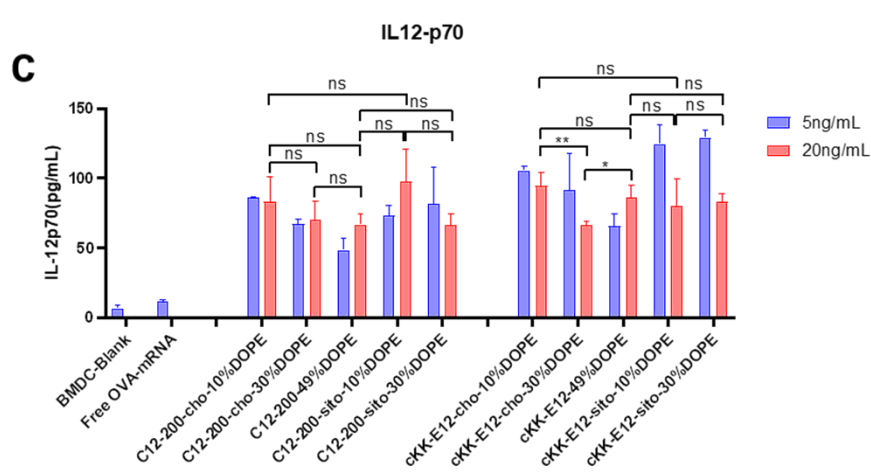
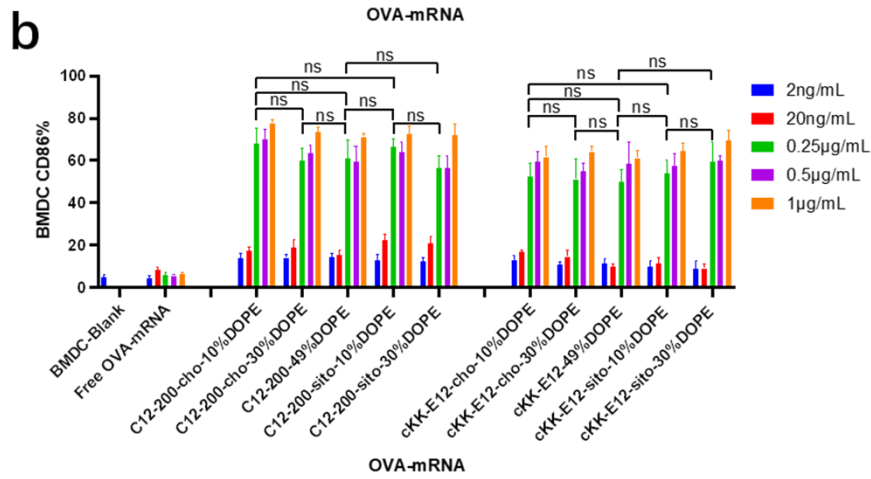
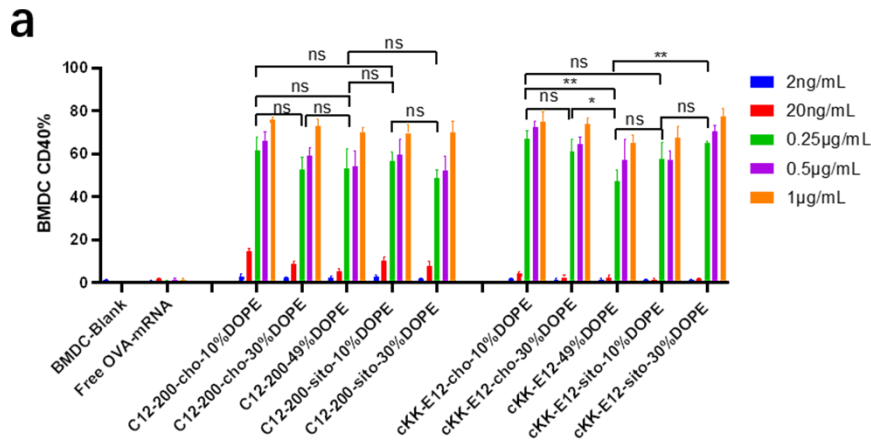
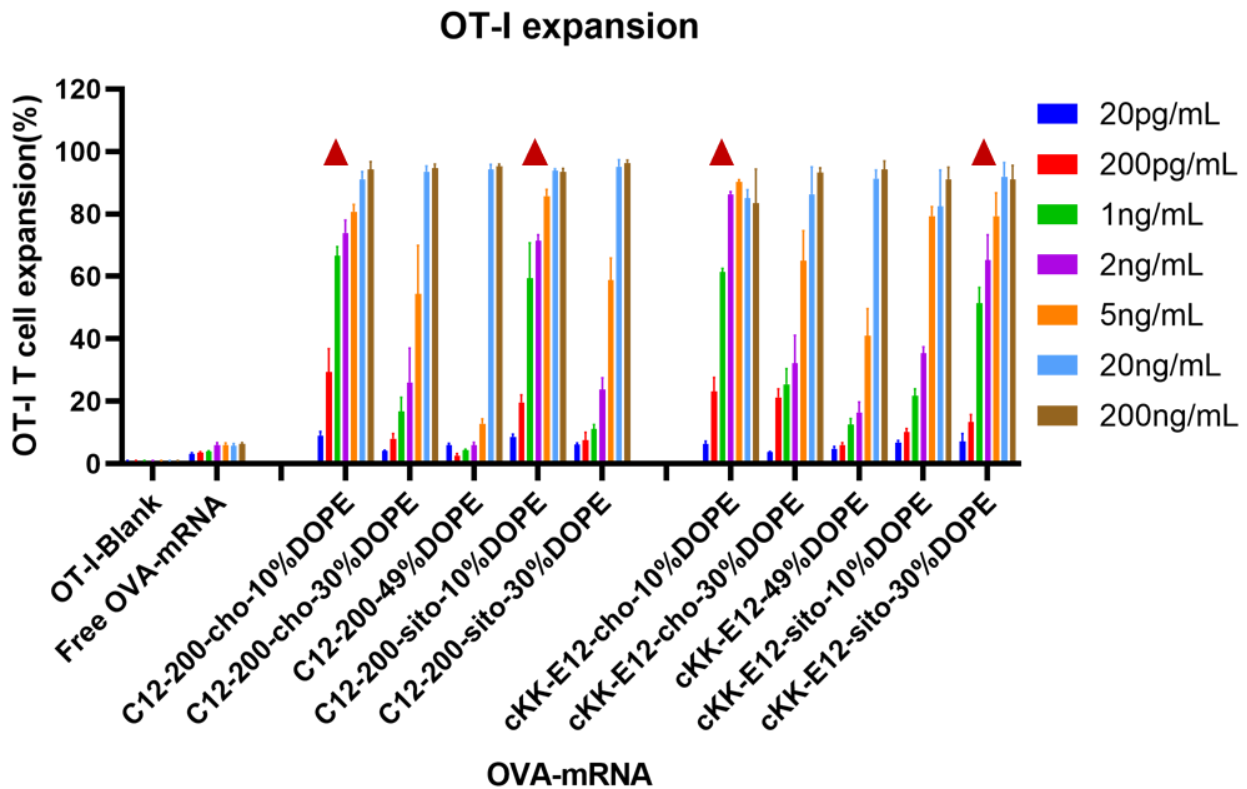


**Figure 4.** LNPs Transfection after encapsulating OVA-mRNA on BMDC cells. **(a)** BMDC activation was monitored through CD40 cellular marker on BMDCs by the different concentrations of LNPs. **(b)** BMDCs activation was monitored through CD86 cellular marker on BMDCs by the different concentrations of LNPs. **(c)** Cytokine IL-12 (p70) expression from BMDCs' supernatant. **(d)** Cell viability of BMDCs with different concentrations of LNPs, dotted line represents 60% cell viability. Data are presented as mean  $\pm$  sd. Statistical significance was calculated by unpaired student t-test on 0.25  $\mu$ g/mL **(a-b)**, 20 ng/mL **(c)**. (\*\*\*\*,  $P < 0.0001$ , \*\*\*,  $P < 0.001$ , \*\*,  $P < 0.01$ , \*,  $P < 0.05$ , ns, no significant difference,  $n = 3$ )

### **CD8<sup>+</sup> T-cell expansion by LNPs and cytokine production**

The goal of tumor and viral vaccination is to expand antigen-specific CD8<sup>+</sup> T cells through priming by APCs, creating a large pool of cytotoxic effector T cells that migrate through the body to clear tumors or infections.<sup>35-37</sup> Therefore, we evaluated OVA-specific T cell expansion induced by different LNPs. BMDCs were incubated with LNPs for 4 h, followed by the addition of CD8<sup>+</sup> (OT-I) T-cells, and the mixed cells were co-cultured for another 72 h.

All LNPs induced potent OT-I proliferation in a mRNA concentration-dependent manner, which was significantly stronger than the blank and free OVA-mRNA groups (**Fig. 5**). T cell proliferation was negligible in the lowest concentration (200 pg/mL), while it plateaued at ~90% with an OVA-mRNA concentration of 20 ng/mL. Next, we investigated the proliferation differences of LNPs in the middle mRNA concentration range. We observed that the C12-200-cho-10%DOPE, C12-200-sito-10%DOPE, cKK-E12-cho-10%DOPE and cKK-E12-sito-30%DOPE LNP formulations induced a potent OT-I T cell stimulation with 1 ng/mL of OVA-mRNA. This indicates these four LNP formulations are able to elicit a robust T cell proliferation even at low OVA-mRNA concentrations, which could serve as efficient LNP candidates eliciting potent T cell responses.

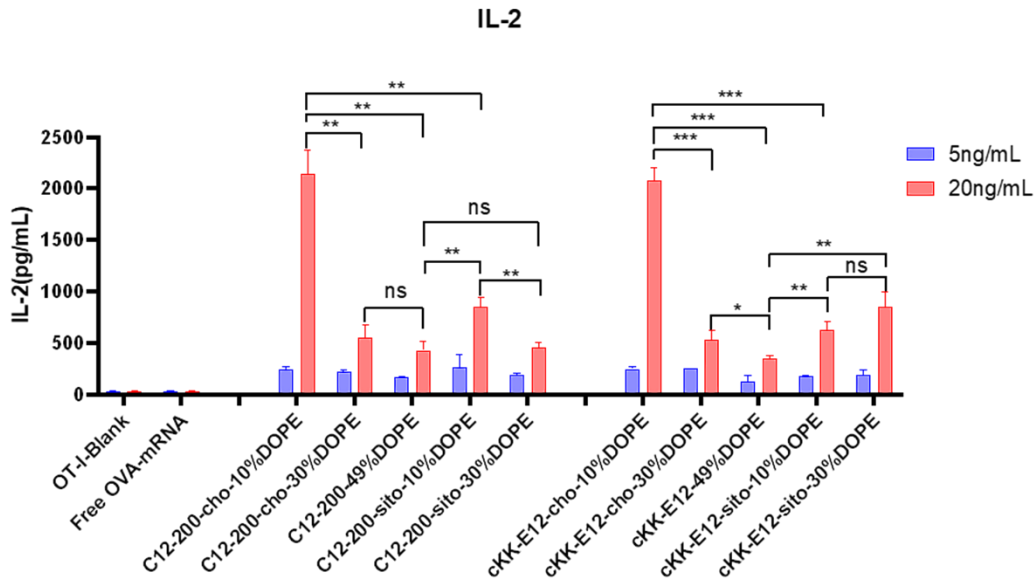
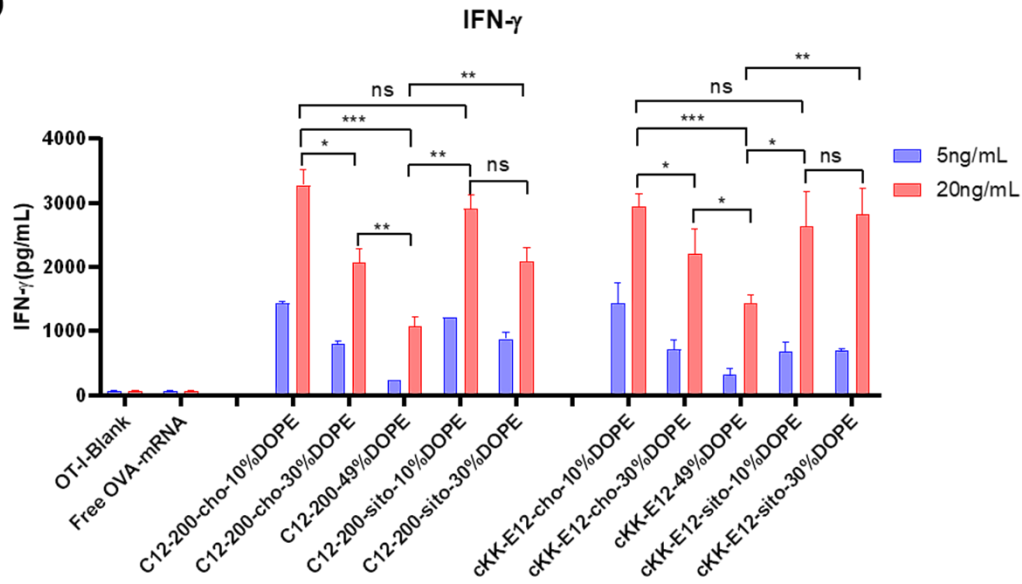
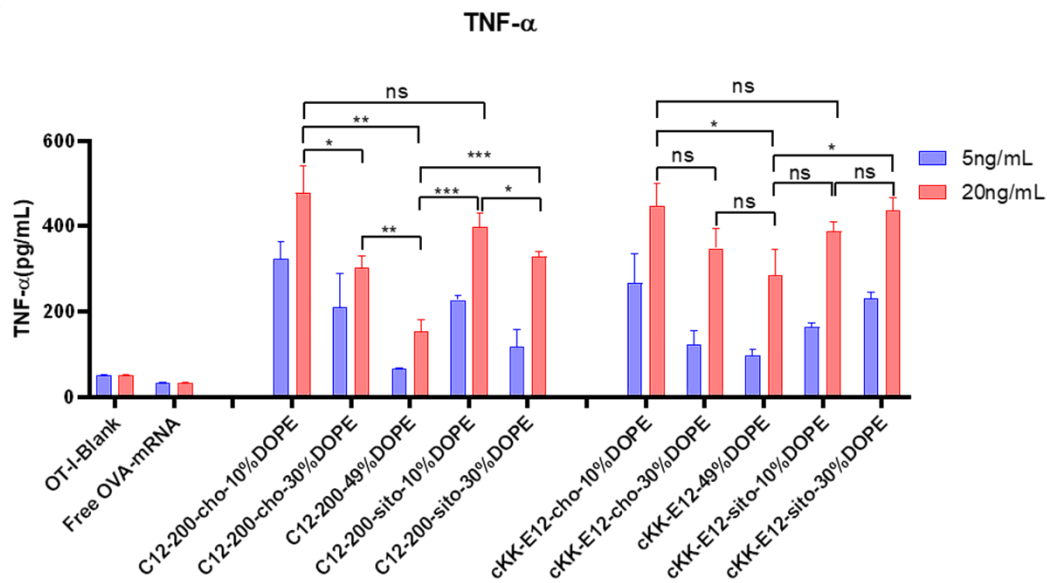


**Figure 5.** OT-I T cell expansion of LNPs with different OVA-mRNA concentrations. Triangle represents the four leading LNP candidates that induced superior OT-I responses when compared at 1 ng/mL.

### Cytokine production of T cell supernatant

When T cells divide and differentiate into effector T cells, cytokines like IFN- $\gamma$ , TNF- $\alpha$ , and cytotoxic proteins such as granzymes and perforin are simultaneously induced in response to acute infection.<sup>38</sup> Proinflammatory cytokines, such as interleukin-2 (IL-2), are pivotal for the proliferation of T cells and the generation of effector and memory cells.<sup>39,40</sup> Activated CD8<sup>+</sup> T cells possess superior effector functions when cultured in a high concentration of IL-2 compared to cells cultured in low concentrations of this cytokine.<sup>41</sup> Therefore, we quantified the expression of IL-2, IFN- $\gamma$ , and TNF- $\alpha$  in OT-I cells in the culture supernatant 72 h after LNP stimulation using an ELISA assay (**Fig. 6a-6c**). The cytokines were significantly upregulated after treating cells with LNPs as compared to non-treated or free OVA-mRNA treated cells. Differences in cytokine production among the evaluated LNPs were determined at two mRNA concentrations (5 and 20 ng/mL). Consistent with OT-I cell proliferation data, replacing cholesterol with  $\beta$ -sitosterol did not boost the T cell response and cytokine production for LNPs with C12-200. The increased molar ratio of fusogenic helper lipid DOPE in C12-200 LNPs neither enhanced the T cell response nor cytokine IL-2 production. The increased molar ratio of DOPE did not enhance the cytokine IL-2 production for cKK-E12 LNPs, and it only showed some enhancement in cytokine IL-2 production at 30% DOPE but decreased at 49% DOPE for cKK-E12 LNPs using  $\beta$ -sitosterol. On the other hand, for Th1 cytokine (IFN- $\gamma$ ) and proinflammatory cytokines (TNF- $\alpha$ ) production, we also observed that C12-200-cho-10%DOPE, C12-200-sito-10%DOPE, cKK-E12-cho-10%DOPE and cKK-E12-sito-30%DOPE LNP formulations triggered higher IFN- $\gamma$  and TNF- $\alpha$  levels in the OT-I T cell supernatant. Taken together, these results showed that four LNP formulations (*i.e.* C12-200-cho-10%DOPE, C12-200-sito-

10%DOPE, cKK-E12-cho-10%DOPE and cKK-E12-sito-30%DOPE) induced a potent T cell proliferation and concomitant inflammatory cytokine production.

**a****b****c**

**Figure 6.** Cytokine production levels of (a) IL-2, (b) IFN- $\gamma$ , (c) TNF- $\alpha$  in culture media of OT-I T cells by different LNPs, measured by ELISA. Data are presented as mean  $\pm$  sd. Statistical significance was calculated by unpaired student t-test on 20 ng/mL. (\*\*\*\*,  $P < 0.0001$ , \*\*\*,  $P < 0.001$ , \*\*,  $P < 0.01$ , \*,  $P < 0.05$ , ns, no significant difference,  $n = 3$ )

## Conclusion

We investigated a small library of LNP formulations to deliver mRNA into BMDCs and evaluate T cell activation towards the development of LNP-mRNA vaccine candidates. LNPs have been validated as effective and well-tolerated on mRNA delivery and recognized as an exceptional mRNA vaccine vector. Proper LNP vaccine candidate screening is essential to identify superior LNP formulations that could boost robust T cell proliferation. It has been reported that replacing cholesterol with  $\beta$ -sitosterol or fusogenic DOPE could enhance transfection efficiency. We discovered that the introduction of  $\beta$ -sitosterol only exerted enhanced transfection in LNPs using MC3 as the ionizable lipid, while exhibiting varied transfection efficiency effects on different cell lines when C12-200 and cKK-E12 were used. Replacing cholesterol with DOPE resulted in mixed mRNA transfection efficiencies in different cells. This may be due to the enhanced transfection efficiency requiring different helper lipids ratios when using different ionizable lipids of LNPs, and also the mechanism of mRNA release into cytoplasm seems to be cell type-dependent. We demonstrated that the LNP-mRNA vaccine candidates can generate significant activation of BMDCs, robust T cell proliferation, and enhanced cytokine production *ex vivo*. We identified four LNP formulations (C12-200-cho-10%DOPE, C12-200-sito-10%DOPE, cKK-E12-cho-10%DOPE, and cKK-E12-sito-30%DOPE) which exhibit efficient T cell expansion and cytokines production and these will be tested in a future *in vivo* study towards the development of a cancer vaccine.

## Methods

### Chemicals

All lipids, 1,2-dioleoyl-*sn*-glycero-3-phosphoethanolamine (DOPE), 1,2-distearoyl-*sn*-glycero-3-phosphocholine (DSPC), 1,2-dimyristoyl-*rac*-glycero-3-methoxypolyethylene glycol-2000 (DMG-PEG2K) were purchased from Avanti Polar Lipids, DLin-MC3-DMA was purchased from Biorbyt company (Cambridge, England), Hoechst 33342, cholesterol and  $\beta$ -sitosterol was purchased from Sigma-Aldrich. Triton™ X-100 was purchased from Acros Organics. QuantiT™ RiboGreen® RNA reagent and rRNA standards were purchased from Life Technologies. Clean cap EGFP-mRNA (5moU) and OVA-mRNA (5moU) were purchased from Trilink biotechnology. C12-200 and cKK-E12 lipids were synthesized according to the literatures.<sup>28, 29</sup> The following antibodies were used for flow cytometry: anti-Thy1.2 PeCy7, anti-CD8 efluor450, anti-CD25 APC, Live/Dead stain and purchased from BD Bioscience. CD4 and CD8 T-cell isolation kits were purchased from Miltenyi (Leiden, Netherlands).

### Cell culture

THP-1, RAW264.7, HeLa, Calu-3 cells were obtained from ATCC. DC2.4 is a murine dendritic cell line kindly provided by Kenneth Rock, University of Massachusetts Medical School, Worcester, MA. Cells were maintained either in DMEM or RPMI 1640 (Thermo Fisher Scientific) supplemented with 10% fetal bovine serum (FBS) (Gibco) and 1% penicillin-streptomycin antibiotic (Gibco). Cell culture and all biological experiments were performed at 37 °C in 5% CO<sub>2</sub> conditions in a cell culture incubator.

6 to 8-week-old female mice (C57BL/6 mice were used to isolate BMDCs. Briefly, the femur and tibia from mice hind legs were collected and bone marrow cells were flushed out with PBS using a syringe. Cells were resuspended into RPMI1640 medium with 10% FBS, antibiotics, and  $\beta$ -mercaptoethanol (55  $\mu$ M, Gibco). Cells were grown with a supplement of recombinant murine granulocyte-macrophage-colony-stimulating factor (GM-CSF) (20 ng/mL, Peprotech). The cell culture medium was refreshed every other day.

### Mouse experiments

C57BL/6, OT-I transgenic mice on a C57BL/6 background were purchased from Jackson Laboratory (CA, USA), bred in-house under standard laboratory conditions, and provided with food and water ad libitum. All animal experiments were performed in compliance with the Dutch government guidelines and the Directive 2010/63/EU of the European Parliament. Experiments were approved by the Ethics Committee for Animal Experiments of Leiden University.

### LNP-mRNA preparation and characterization

Lipids were combined at the desired molar ratios and concentrations from stock solutions dissolved in chloroform. Solvents were evaporated under a nitrogen flow and residual solvent was removed in vacuo for at least 30 minutes. The lipid film was dissolved in absolute ethanol (total lipids was 0.4  $\mu$ mol) and used for the assembly. A solution of mRNA was made by diluting mRNA (EGFP-mRNA, OVA-mRNA) in 50 mM citrate buffer (pH = 4, RNase free). The solutions were loaded into two separate syringes and connected to a T-junction microfluidic mixer. The solutions were mixed in a 3:1 flow ratio of mRNA against lipids (1.5 mL/min for mRNA solution, 0.5 mL/min for lipids solution,

lipids: mRNA (wt/wt) =40:1). After mixing, the solution was directly loaded in a 20 kDa MWCO dialysis cassette (Slide-A-Lyzer™, Thermo Scientific) and dialyzed against 1 x PBS overnight. The size and zeta potential of LNPs were measured using dynamic light scattering (DLS, Malvern) and Zetasizer (Malvern). Long term stability of LNPs was assessed by measuring the hydrodynamic radius using DLS for 1 month.

The encapsulation efficiency (EE) of mRNA was determined by Quant-iT™ RiboGreen™ RNA Assay Kit (Invitrogen). For the determination of non-encapsulated mRNA, LNPs after dialysis were diluted with 1 x TE buffer (RNase free) and treated with the RiboGreen™ reagent. For the determination of the total amount of mRNA, LNPs after dialysis were treated with 1% Triton X-100 in TE buffer (RNase free) and incubated for 5 minutes followed by dilution with TE buffer and treatment with the RiboGreen™ reagent. The supplied RNA standards were used to generate a standard curve and changes in fluorescence was measured in 96-well plates using a TECAN Infinite M1000 Pro microplate reader. The percentage of mRNA encapsulation (EE%) was determined using the fraction of  $(F_{\text{total RNA}} - F_{\text{free RNA}})/F_{\text{total RNA}} * 100\%$ .

### ***In vitro* GFP protein expression of LNPs**

Briefly, HeLa, and Calu-3, DC2.4, THP-1 and RAW264.7 cells were seeded in 96-well plates at a density of  $1 \times 10^4$  cells/well and cultured at 37 °C in 5% CO<sub>2</sub> overnight. Then cells were transfected with LNPs containing different concentrations of EGFP-mRNA overnight (0.1 µg/mL, 0.25 µg/mL, 0.5 µg/mL, 1 µg/mL). The expression of GFP protein was quantified by flow cytometry. Data analysis was performed using the FlowJo Software version 7.6. For confocal microscopy, DC2.4 cells were seeded on the 8-well confocal slide at a density of  $5 \times 10^4$  cells/well and cultured overnight, then LNPs were added and incubated overnight (1 µg/mL), after that Hoechst 33342 (5 µM) was added and incubated for 1 h before confocal microscopy imaging (Leica TCS SP8 confocal laser scanning microscope).

### **BMDC transfection**

Bone marrow-derived dendritic cells (BMDCs) were isolated from murine tibia and femurs of C57BL/6 mice. Bone marrow cells were stimulated for 10 days with 20 ng/mL GM-CSF in complete IMDM (supplemented with 100 U/mL PenStrep, 2 mM glutaMAX and 10% FCS). After 10 days of culture, 20,000 BMDCs were plated in 96-well plates (Greiner Bio-One B.V., Alphen aan den Rijn, Netherlands) and different LNPs encapsulating EGFP-mRNA were added at varying concentrations and incubated with BMDC overnight (0.25 µg/mL, 0.5 µg/mL, 1 µg/mL). Cells were analyzed by flow cytometry (CytoFLEX S, Beckman Coulter, CA, USA). Data were analyzed by using FlowJo software (Treestar, OR, USA). For confocal microscopy, BMDCs were seeded on the 8-well confocal slide at a density of  $5 \times 10^4$  cells/well and cultured overnight, then LNPs were added and incubated overnight (0.5 µg/mL), then followed with confocal microscopy measurement (Leica TCS SP8 confocal laser scanning microscope).

### **BMDC activation**

Bone marrow-derived dendritic cells (BMDCs) were isolated and cultured described as above. After 10 days, different LNPs containing OVA-mRNA were added to the BMDC cells and incubated overnight (2 ng/mL, 20 ng/mL, 0.25 µg/mL 0.5 µg/mL, 1 µg/mL). After 24 h of incubation, cells were collected and followed immunostaining of CD40 and CD86 to quantify the expression by flow

cytometry. Data analysis was performed using the FlowJo Software version 7.6. The supernatant was collected for measuring the expression level of cytokine (IL12-p70) by ELISA.

### ***Ex vivo* T-cell expansion**

Wild-type (WT) BMDCs were cultured as described above, after 10 days, the BMDCs (20,000 cells per well) were exposed to the different LNP formulations with various concentrations (20 pg/mL, 200 pg/mL, 1 ng/mL, 2 ng/mL, 5 ng/mL, 20 ng/mL, 200 ng/mL). Meanwhile, spleens were removed from OT-I mice and strained through a 70- $\mu$ m cell strainer to obtain a single-cell suspension. Erythrocytes were lysed with Ammonium-Chloride-Potassium (ACK) lysis buffer (0.15M NH<sub>4</sub>Cl, 1mM KHCO<sub>3</sub>, 0.1mM Na<sub>2</sub>EDTA; pH 7.3). CD8<sup>+</sup> T cells were isolated using a CD8<sup>+</sup> T cell isolation kit (Miltenyi Biotec B.V., Leiden, Netherlands) according to the manufacturer's protocol. After 4 h of LNP incubation, the BMDCs were centrifuged, the supernatant medium was removed, and replaced with 60,000 CD8<sup>+</sup> T-cells to obtain a number ratio of 3:1 CD8<sup>+</sup> T cells:BMDCs. Co-cultures were cultured for 72 h in complete RPMI 1640 medium supplemented with 2 mM glutamine, 10% FCS, 100 U/mL penicillin/streptomycin, and 50  $\mu$ M  $\beta$ -mercaptoethanol. After 72 h, the cell suspension was stained for anti-Thy1.2 PeCy7, anti-CD8 efluor450, anti-CD25 APC, Live/Dead stain indicating cell viability, and then analyzed by flow cytometry (CytoFLEX S, Beckman Coulter, CA, USA). The supernatant was collected for measuring the expression levels of cytokines by ELISA.

### **ELISA measurements of OT-I T cell supernatant**

Cytokines (IL-2, IFN- $\gamma$ , and TFN- $\alpha$ ) from OT-I T cell supernatants were detected by individual cytokine ELISA kits according to the manufacturer's instructions (BD Biosciences). In brief, the assay plate was coated with 50  $\mu$ l/well of capture antibody (IL-2, IFN- $\gamma$ , and TFN- $\alpha$ , respectively) in coating buffer, covered and incubated overnight at 4 °C. Next, the plate was washed (3x) with wash buffer (PBS with 0.05% Tween-20) and blocked with 100  $\mu$ l/well of assay diluent (PBS with 10%FCS) and incubated for 1 hour at RT. The plate was washed (3x) with wash buffer and 50  $\mu$ L/well (diluted) samples/standard/blank was added incubated for 2 hours at RT. Next, the plate was washed (3x) with wash buffer and 50  $\mu$ L/well of the working detector (Detection AB + Sav-HRP reagent) was added and incubated for another 1 hour at RT. After washing the plate (5X) with wash buffer, 50  $\mu$ L/well substrate solution was added and incubate for 15-30min at RT in the dark. Finally, 25  $\mu$ l/well stop solution was added and the absorbance at 450 nm was measured within 30 minutes.

### **Statistical analyses**

Statistical analyses were performed with Prism 8 (GraphPad). Data were compared using unpaired student t-test analysis. (\*\*\*\*, P < 0.0001, \*\*\*, P < 0.001, \*\*, P < 0.01, \*, P < 0.05, ns, no significant difference, n = 3)

## **References**

1. Thess, A.; Grund, S.; Mui, B. L.; Hope, M. J.; Baumhof, P.; Fotin-Mleczek, M.; Schlake, T., Sequence-engineered mRNA Without Chemical Nucleoside Modifications Enables an Effective Protein Therapy in Large Animals. *Molecular Therapy* **2015**, *23* (9), 1456-1464.
2. Sahin, U.; Karikó, K.; Türeci, Ö., mRNA-based therapeutics — developing a new class of drugs. *Nature Reviews Drug Discovery* **2014**, *13* (10), 759-780.

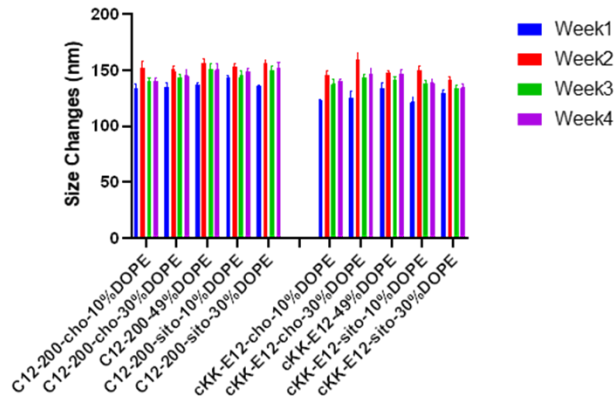
3. Oberli, M. A.; Reichmuth, A. M.; Dorkin, J. R.; Mitchell, M. J.; Fenton, O. S.; Jaklenec, A.; Anderson, D. G.; Langer, R.; Blankschtein, D., Lipid Nanoparticle Assisted mRNA Delivery for Potent Cancer Immunotherapy. *Nano Letters* **2017**, *17* (3), 1326-1335.
4. Cheng, Q.; Wei, T.; Farbiak, L.; Johnson, L. T.; Dilliard, S. A.; Siegwart, D. J., Selective organ targeting (SORT) nanoparticles for tissue-specific mRNA delivery and CRISPR–Cas gene editing. *Nature Nanotechnology* **2020**, *15* (4), 313-320.
5. Billingsley, M. M.; Singh, N.; Ravikumar, P.; Zhang, R.; June, C. H.; Mitchell, M. J., Ionizable Lipid Nanoparticle-Mediated mRNA Delivery for Human CAR T Cell Engineering. *Nano Letters* **2020**, *20* (3), 1578-1589.
6. Pardi, N.; Hogan, M. J.; Porter, F. W.; Weissman, D., mRNA vaccines — a new era in vaccinology. *Nature Reviews Drug Discovery* **2018**, *17* (4), 261-279.
7. Guan, S.; Rosenecker, J., Nanotechnologies in delivery of mRNA therapeutics using nonviral vector-based delivery systems. *Gene Therapy* **2017**, *24* (3), 133-143.
8. Karikó, K.; Muramatsu, H.; Welsh, F. A.; Ludwig, J.; Kato, H.; Akira, S.; Weissman, D., Incorporation of Pseudouridine Into mRNA Yields Superior Nonimmunogenic Vector With Increased Translational Capacity and Biological Stability. *Molecular Therapy* **2008**, *16* (11), 1833-1840.
9. Sabnis, S.; Kumarasinghe, E. S.; Salerno, T.; Mihai, C.; Ketova, T.; Senn, J. J.; Lynn, A.; Bulychev, A.; McFadyen, I.; Chan, J.; Almarsson, Ö.; Stanton, M. G.; Benenato, K. E., A Novel Amino Lipid Series for mRNA Delivery: Improved Endosomal Escape and Sustained Pharmacology and Safety in Non-human Primates. *Molecular Therapy* **2018**, *26* (6), 1509-1519.
10. Yin, H.; Kanasty, R. L.; Eltoukhy, A. A.; Vegas, A. J.; Dorkin, J. R.; Anderson, D. G., Non-viral vectors for gene-based therapy. *Nature Reviews Genetics* **2014**, *15* (8), 541-555.
11. Akinc, A.; Maier, M. A.; Manoharan, M.; Fitzgerald, K.; Jayaraman, M.; Barros, S.; Ansell, S.; Du, X.; Hope, M. J.; Madden, T. D.; Mui, B. L.; Semple, S. C.; Tam, Y. K.; Ciufolini, M.; Witzigmann, D.; Kulkarni, J. A.; van der Meel, R.; Cullis, P. R., The Onpattro story and the clinical translation of nanomedicines containing nucleic acid-based drugs. *Nature Nanotechnology* **2019**, *14* (12), 1084-1087.
12. Kowalski, P. S.; Rudra, A.; Miao, L.; Anderson, D. G., Delivering the Messenger: Advances in Technologies for Therapeutic mRNA Delivery. *Molecular Therapy* **2019**, *27* (4), 710-728.
13. Semple, S. C.; Akinc, A.; Chen, J.; Sandhu, A. P.; Mui, B. L.; Cho, C. K.; Sah, D. W. Y.; Stebbing, D.; Crosley, E. J.; Yaworski, E.; Hafez, I. M.; Dorkin, J. R.; Qin, J.; Lam, K.; Rajeev, K. G.; Wong, K. F.; Jeffs, L. B.; Nechev, L.; Eisenhardt, M. L.; Jayaraman, M.; Kazem, M.; Maier, M. A.; Srinivasulu, M.; Weinstein, M. J.; Chen, Q.; Alvarez, R.; Barros, S. A.; De, S.; Klimuk, S. K.; Borland, T.; Kosovrasti, V.; Cantley, W. L.; Tam, Y. K.; Manoharan, M.; Ciufolini, M. A.; Tracy, M. A.; de Fougères, A.; MacLachlan, I.; Cullis, P. R.; Madden, T. D.; Hope, M. J., Rational design of cationic lipids for siRNA delivery. *Nature Biotechnology* **2010**, *28* (2), 172-176.
14. Wang, C.; Zhang, Y.; Dong, Y., Lipid Nanoparticle–mRNA Formulations for Therapeutic Applications. *Accounts of Chemical Research* **2021**, *54* (23), 4283-4293.
15. Verbeke, R.; Lentacker, I.; De Smedt, S. C.; Dewitte, H., The dawn of mRNA vaccines: The COVID-19 case. *Journal of Controlled Release* **2021**, *333*, 511-520.
16. Miao, L.; Li, L.; Huang, Y.; Delcassian, D.; Chahal, J.; Han, J.; Shi, Y.; Sadtler, K.; Gao, W.; Lin, J.; Doloff, J. C.; Langer, R.; Anderson, D. G., Delivery of mRNA vaccines with heterocyclic lipids increases anti-tumor efficacy by STING-mediated immune cell activation. *Nature Biotechnology* **2019**, *37* (10), 1174-1185.
17. Klichinsky, M.; Ruella, M.; Shestova, O.; Lu, X. M.; Best, A.; Zeeman, M.; Schmierer, M.; Gabrusiewicz, K.; Anderson, N. R.; Petty, N. E.; Cummins, K. D.; Shen, F.; Shan, X.; Veliz, K.; Blouch, K.; Yashiro-Ohtani, Y.; Kenderian, S. S.; Kim, M. Y.; O'Connor, R. S.; Wallace, S. R.;

- Kozlowski, M. S.; Marchione, D. M.; Shestov, M.; Garcia, B. A.; June, C. H.; Gill, S., Human chimeric antigen receptor macrophages for cancer immunotherapy. *Nature Biotechnology* **2020**, *38* (8), 947-953.
18. Richner, J. M.; Himansu, S.; Dowd, K. A.; Butler, S. L.; Salazar, V.; Fox, J. M.; Julander, J. G.; Tang, W. W.; Shresta, S.; Pierson, T. C.; Ciaramella, G.; Diamond, M. S., Modified mRNA Vaccines Protect against Zika Virus Infection. *Cell* **2017**, *168* (6), 1114-1125.e10.
19. Pardi, N.; Hogan, M. J.; Pelc, R. S.; Muramatsu, H.; Andersen, H.; DeMaso, C. R.; Dowd, K. A.; Sutherland, L. L.; Scarce, R. M.; Parks, R.; Wagner, W.; Granados, A.; Greenhouse, J.; Walker, M.; Willis, E.; Yu, J.-S.; McGee, C. E.; Sempowski, G. D.; Mui, B. L.; Tam, Y. K.; Huang, Y.-J.; Vanlandingham, D.; Holmes, V. M.; Balachandran, H.; Sahu, S.; Lifton, M.; Higgs, S.; Hensley, S. E.; Madden, T. D.; Hope, M. J.; Karikó, K.; Santra, S.; Graham, B. S.; Lewis, M. G.; Pierson, T. C.; Haynes, B. F.; Weissman, D., Zika virus protection by a single low-dose nucleoside-modified mRNA vaccination. *Nature* **2017**, *543* (7644), 248-251.
20. VanBlargan, L. A.; Himansu, S.; Foreman, B. M.; Ebel, G. D.; Pierson, T. C.; Diamond, M. S., An mRNA Vaccine Protects Mice against Multiple Tick-Transmitted Flavivirus Infections. *Cell Reports* **2018**, *25* (12), 3382-3392.e3.
21. Pardi, N.; Secreto, A. J.; Shan, X.; Debonera, F.; Glover, J.; Yi, Y.; Muramatsu, H.; Ni, H.; Mui, B. L.; Tam, Y. K.; Shaheen, F.; Collman, R. G.; Karikó, K.; Danet-Desnoyers, G. A.; Madden, T. D.; Hope, M. J.; Weissman, D., Administration of nucleoside-modified mRNA encoding broadly neutralizing antibody protects humanized mice from HIV-1 challenge. *Nature Communications* **2017**, *8* (1), 14630.
22. Pardi, N.; LaBranche, C. C.; Ferrari, G.; Cain, D. W.; Tombácz, I.; Parks, R. J.; Muramatsu, H.; Mui, B. L.; Tam, Y. K.; Karikó, K.; Polacino, P.; Barbosa, C. J.; Madden, T. D.; Hope, M. J.; Haynes, B. F.; Montefiori, D. C.; Hu, S.-L.; Weissman, D., Characterization of HIV-1 Nucleoside-Modified mRNA Vaccines in Rabbits and Rhesus Macaques. *Molecular Therapy - Nucleic Acids* **2019**, *15*, 36-47.
23. Pardi, N.; Parkhouse, K.; Kirkpatrick, E.; McMahon, M.; Zost, S. J.; Mui, B. L.; Tam, Y. K.; Karikó, K.; Barbosa, C. J.; Madden, T. D.; Hope, M. J.; Krammer, F.; Hensley, S. E.; Weissman, D., Nucleoside-modified mRNA immunization elicits influenza virus hemagglutinin stalk-specific antibodies. *Nature Communications* **2018**, *9* (1), 3361.
24. Freyn, A. W.; Ramos da Silva, J.; Rosado, V. C.; Bliss, C. M.; Pine, M.; Mui, B. L.; Tam, Y. K.; Madden, T. D.; de Souza Ferreira, L. C.; Weissman, D.; Krammer, F.; Coughlan, L.; Palese, P.; Pardi, N.; Nachbagauer, R., A Multi-Targeting, Nucleoside-Modified mRNA Influenza Virus Vaccine Provides Broad Protection in Mice. *Molecular Therapy* **2020**, *28* (7), 1569-1584.
25. Bahl, K.; Senn, J. J.; Yuzhakov, O.; Bulychev, A.; Brito, L. A.; Hassett, K. J.; Laska, M. E.; Smith, M.; Almarsson, Ö.; Thompson, J.; Ribeiro, A.; Watson, M.; Zaks, T.; Ciaramella, G., Preclinical and Clinical Demonstration of Immunogenicity by mRNA Vaccines against H10N8 and H7N9 Influenza Viruses. *Molecular Therapy* **2017**, *25* (6), 1316-1327.
26. Patel, S.; Ashwanikumar, N.; Robinson, E.; Xia, Y.; Mihai, C.; Griffith, J. P.; Hou, S.; Esposito, A. A.; Ketova, T.; Welscher, K.; Joyal, J. L.; Almarsson, Ö.; Sahay, G., Naturally-occurring cholesterol analogues in lipid nanoparticles induce polymorphic shape and enhance intracellular delivery of mRNA. *Nature Communications* **2020**, *11* (1), 983.
27. Kulkarni, J. A.; Witzigmann, D.; Leung, J.; van der Meel, R.; Zaifman, J.; Darjuan, M. M.; Grisch-Chan, H. M.; Thöny, B.; Tam, Y. Y. C.; Cullis, P. R., Fusion-dependent formation of lipid nanoparticles containing macromolecular payloads. *Nanoscale* **2019**, *11* (18), 9023-9031.
28. Love, K. T.; Mahon, K. P.; Levins, C. G.; Whitehead, K. A.; Querbes, W.; Dorkin, J. R.; Qin, J.; Cantley, W.; Qin, L. L.; Racie, T.; Frank-Kamenetsky, M.; Yip, K. N.; Alvarez, R.; Sah, D. W. Y.; de Fogerolles, A.; Fitzgerald, K.; Koteliensky, V.; Akinc, A.; Langer, R.; Anderson, D. G., Lipid-like materials

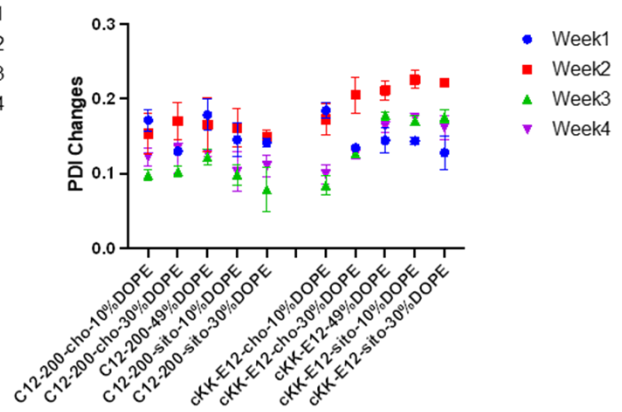
- for low-dose, in vivo gene silencing. *Proceedings of the National Academy of Sciences* **2010**, *107* (5), 1864-1869.
29. Dong, Y.; Love, K. T.; Dorkin, J. R.; Sirirungruang, S.; Zhang, Y.; Chen, D.; Bogorad, R. L.; Yin, H.; Chen, Y.; Vegas, A. J.; Alabi, C. A.; Sahay, G.; Olejnik, K. T.; Wang, W.; Schroeder, A.; Lytton-Jean, A. K. R.; Siegwart, D. J.; Akinc, A.; Barnes, C.; Barros, S. A.; Carioto, M.; Fitzgerald, K.; Hettinger, J.; Kumar, V.; Novobrantseva, T. I.; Qin, J.; Querbes, W.; Kotliansky, V.; Langer, R.; Anderson, D. G., Lipopeptide nanoparticles for potent and selective siRNA delivery in rodents and nonhuman primates. *Proceedings of the National Academy of Sciences* **2014**, *111* (11), 3955-3960.
30. Kauffman, K. J.; Dorkin, J. R.; Yang, J. H.; Heartlein, M. W.; DeRosa, F.; Mir, F. F.; Fenton, O. S.; Anderson, D. G., Optimization of Lipid Nanoparticle Formulations for mRNA Delivery in Vivo with Fractional Factorial and Definitive Screening Designs. *Nano Letters* **2015**, *15* (11), 7300-7306.
31. Pattipeiluhu, R.; Arias-Alpizar, G.; Basha, G.; Chan, K. Y. T.; Bussmann, J.; Sharp, T. H.; Moradi, M. A.; Sommerdijk, N.; Harris, E. N.; Cullis, P. R.; Kros, A.; Witzigmann, D.; Campbell, F., Anionic Lipid Nanoparticles Preferentially Deliver mRNA to the Hepatic Reticuloendothelial System. *Adv Mater* **2022**, *34* (16), e2201095.
32. Hafez, I. M.; Cullis, P. R., Roles of lipid polymorphism in intracellular delivery. *Advanced Drug Delivery Reviews* **2001**, *47* (2), 139-148.
33. Koltover, I.; Salditt, T.; Rädler, J. O.; Safinya, C. R., An Inverted Hexagonal Phase of Cationic Liposome-DNA Complexes Related to DNA Release and Delivery. *Science* **1998**, *281* (5373), 78-81.
34. Trinchieri, G., Interleukin-12 and the regulation of innate resistance and adaptive immunity. *Nature Reviews Immunology* **2003**, *3* (2), 133-146.
35. O'Sullivan, D.; Pearce, E. L., Expanding the role of metabolism in T cells. *Science* **2015**, *348* (6238), 976-977.
36. Appay, V.; Douek, D. C.; Price, D. A., CD8<sup>+</sup> T cell efficacy in vaccination and disease. *Nature Medicine* **2008**, *14* (6), 623-628.
37. Zhang, N.; Bevan, Michael J., CD8<sup>+</sup> T Cells: Foot Soldiers of the Immune System. *Immunity* **2011**, *35* (2), 161-168.
38. Laidlaw, B. J.; Craft, J. E.; Kaech, S. M., The multifaceted role of CD4(+) T cells in CD8(+) T cell memory. *Nat Rev Immunol* **2016**, *16* (2), 102-111.
39. Boyman, O.; Kovar, M.; Rubinstein, M. P.; Surh, C. D.; Sprent, J., Selective Stimulation of T Cell Subsets with Antibody-Cytokine Immune Complexes. *Science* **2006**, *311* (5769), 1924-1927.
40. Abbas, A. K.; Trotta, E.; R. Simeonov, D.; Marson, A.; Bluestone, J. A., Revisiting IL-2: Biology and therapeutic prospects. *Science Immunology* **2018**, *3* (25), eaat1482.
41. Pipkin, M. E.; Sacks, J. A.; Cruz-Guilloty, F.; Lichtenheld, M. G.; Bevan, M. J.; Rao, A., Interleukin-2 and Inflammation Induce Distinct Transcriptional Programs that Promote the Differentiation of Effector Cytolytic T Cells. *Immunity* **2010**, *32* (1), 79-90.

# Supporting Information

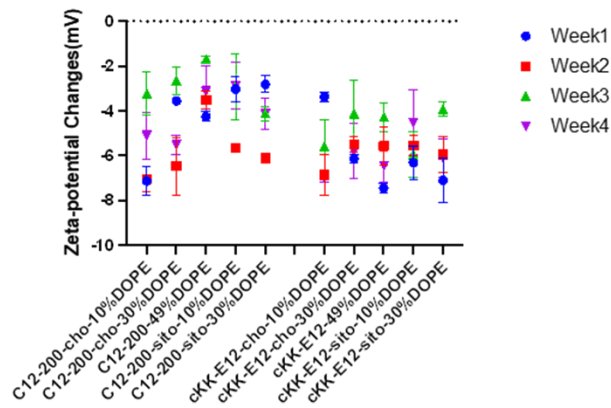
**a**



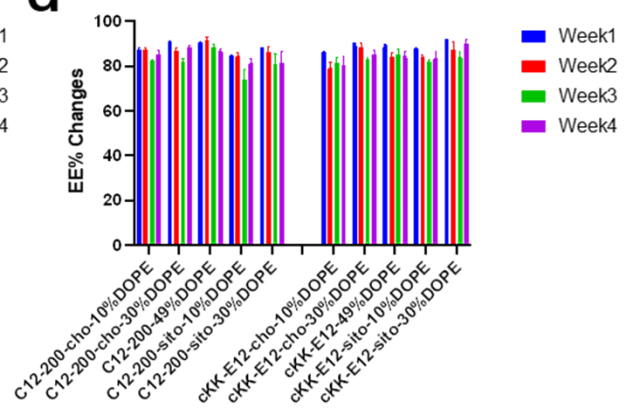
**b**



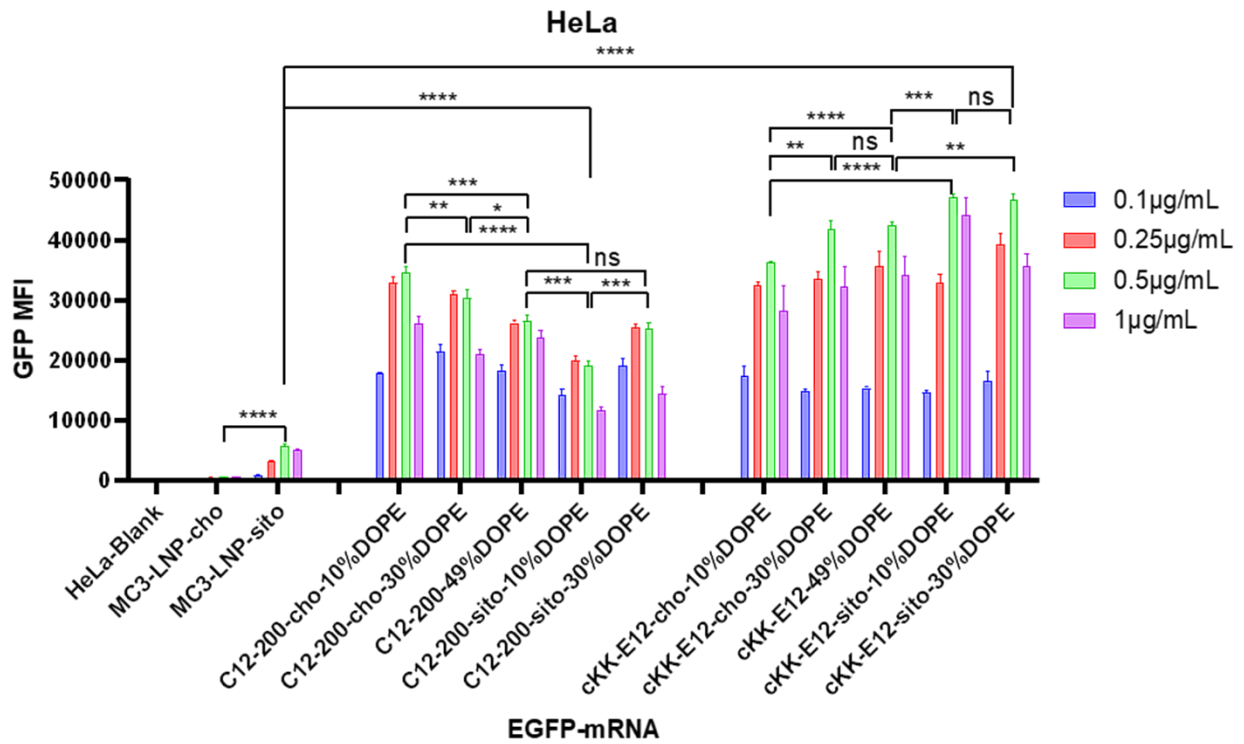
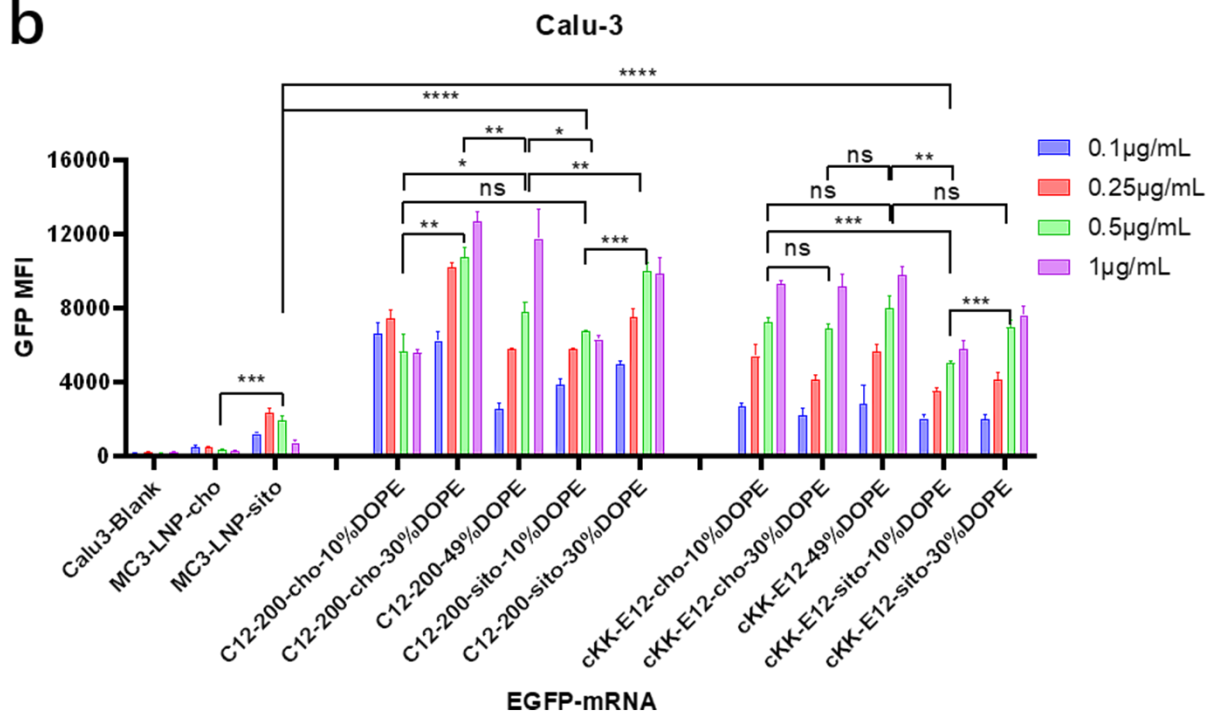
**c**



**d**

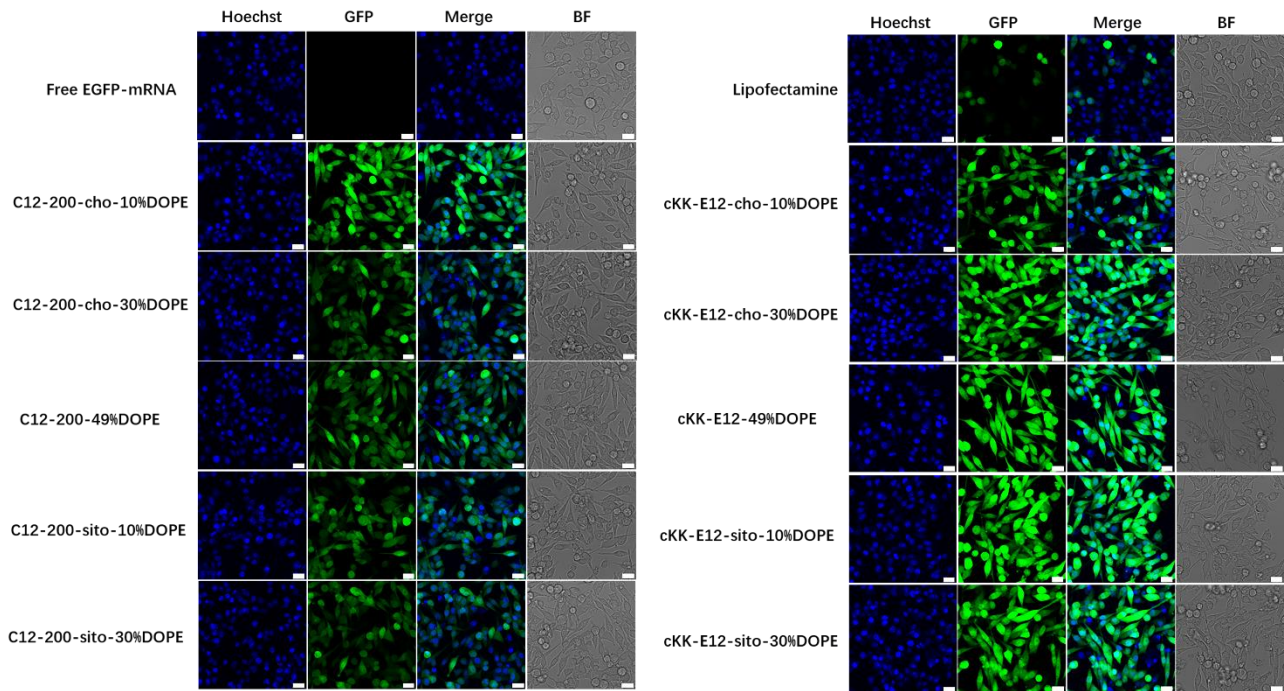


**SI Figure 1.** Stability of LNPs (stored at 4°C). **(a)** Sizes changes, **(b)** PDI changes, **(c)** Zeta potential changes, **(d)** Encapsulation efficiency changes of LNPs over 1 month.

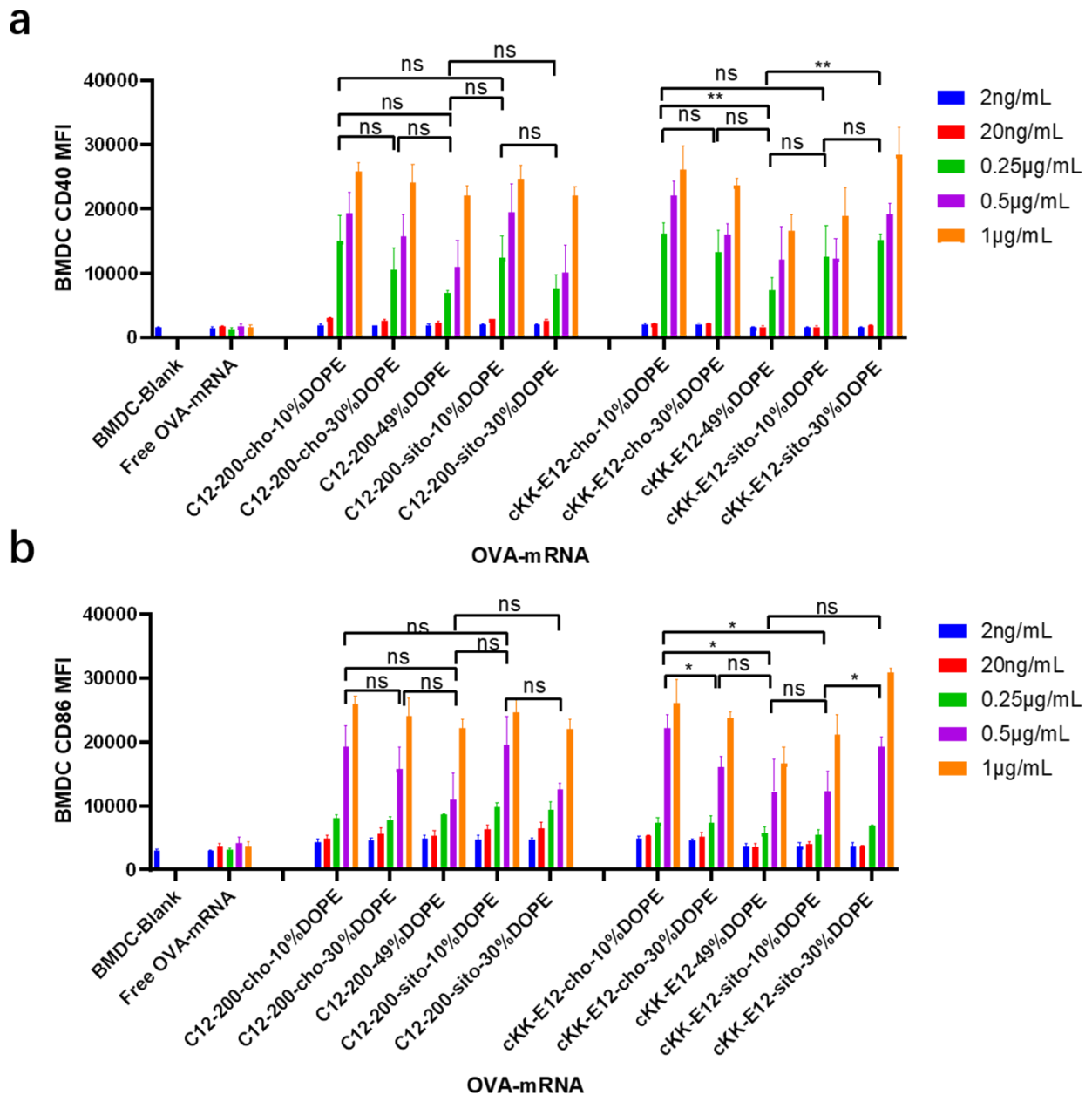
**a****b**

**SI Figure 2.** Transfection efficiency (mean fluorescence intensity, MFI) after encapsulating EGFP-mRNA within (a) HeLa cells and (b) Calu-3 cells. Data are presented as mean  $\pm$  sd. Statistical significance was calculated by unpaired student t-test on 0.5  $\mu$ g/mL. (\*\*\*\*,  $P < 0.0001$ , \*\*\*,  $P < 0.001$ , \*\*,  $P < 0.01$ , \*,  $P < 0.05$ , ns, no significant difference,  $n = 3$ )

DC2.4



**SI Figure 3.** Confocal images of the EGFP-mRNA transfection of LNPs on DC2.4 cells (EGFP-mRNA, 1  $\mu\text{g}/\text{mL}$ , 24 h). Scale bar is 20  $\mu\text{m}$ .



**SI Figure 4.** The mean fluorescence intensities (MFI) of cellular marker CD40 (a) and CD86 (b) after BMDCs activation by the different concentrations of LNPs. Data are presented as mean  $\pm$  sd. Statistical significance was calculated by unpaired student t-test on 0.25  $\mu$ g/mL (a) and 0.5  $\mu$ g/mL (b). (\*\*\*\*,  $P < 0.0001$ , \*\*\*,  $P < 0.001$ , \*\*,  $P < 0.01$ , \*,  $P < 0.05$ , ns, no significant difference,  $n = 3$ )